01 Jan 2016

Antibacterial Properties of Poly (Octanediol Citrate)/gallium-Containing Bioglass Composite Scaffolds

Ehsan Zeimaran

Sara Pourshahrestani

Ivan Djordjevic

Belinda Pingguan-Murphy

et. al. For a complete list of authors, see https://scholarsmine.mst.edu/che_bioeng_facwork/1117

Recommended Citation

E. Zeimaran et al., "Antibacterial Properties of Poly (Octanediol Citrate)/gallium-Containing Bioglass Composite Scaffolds," *Journal of Materials Science: Materials in Medicine*, vol. 27, no. 1, pp. 1 - 11, article no. 18, Springer, Jan 2016.
The definitive version is available at https://doi.org/10.1007/s10856-015-5620-2

J Mater Sci: Mater Med (2016) 27:18
DOI 10.1007/s10856-015-5620-2

DELIVERY SYSTEMS

Original Research

Antibacterial properties of poly (octanediol citrate)/gallium-containing bioglass composite scaffolds

Ehsan Zeimaran[1] · Sara Pourshahrestani[1] · Ivan Djordjevic[1] · Belinda Pingguan-Murphy[1] · Nahrizul Adib Kadri[1] · Anthony W. Wren[2] · Mark R. Towler[1,3]

Received: 9 April 2015 / Accepted: 5 November 2015 / Published online: 16 December 2015

Abstract Bioactive glasses may function as antimicrobial delivery systems through the incorporation and subsequent release of therapeutic ions. The aim of this study was to evaluate the antimicrobial properties of a series of composite scaffolds composed of poly(octanediol citrate) with increased loads of a bioactive glass that releases zinc (Zn^{2+}) and gallium (Ga^{3+}) ions in a controlled manner. The antibacterial activity of these scaffolds was investigated against both Gram-positive (*Staphylococcus aureus*) and Gram-negative (*Escherichia coli*) bacteria. The ability of the scaffolds to release ions and the subsequent ingress of these ions into hard tissue was evaluated using a bovine bone model. Scaffolds containing bioactive glass exhibited antibacterial activity and this increased in vitro with higher bioactive glass loads; viable cells decreased to about 20 % for the composite scaffold containing 30 % bioactive glass. The Ga^{3+} release rate increased as a function of time and Zn^{2+} was shown to incorporate into the surrounding bone.

✉ Mark R. Towler
mtowler@Ryerson.ca

[1] Department of Biomedical Engineering, Faculty of Engineering, University of Malaya, 50603 Kuala Lumpur, Malaysia

[2] Inamori School of Engineering, Alfred University, Alfred, NY, USA

[3] Department of Mechanical and Industrial Engineering, Faculty of Engineering and Architectural Science, Ryerson University, 350 Victoria Street, Toronto, ON M5B 2K3, Canada

1 Introduction

The stiffness and strength of a hard tissue scaffold should be matched with those of natural bone [1]. The mechanical properties of scaffolds are highly dependent on both fabrication technique and porosity; the latter being small enough to facilitate load bearing but large enough to encourage vascularization [2]. Engineered scaffolds for self-regenerative applications not only provide a framework for tissue repair but can also act as carriers for antimicrobial agents. The scaffold should be designed to promote cell adhesion for target tissues whilst also preventing bacterial adhesion and biofilm formation. Infections associated with surgical implants require long periods of antibiotic therapy and usually implant removal and replacement is the only remedy once a mature bacterial biofilm is formed [3].

A biofilm is a microbially derived sessile community characterized by cells that are irreversibly attached to an interface or to one another. Embedded in an extracellular matrix that the attached bacteria have produced, these cells exhibit an altered phenotype with respect to growth rate and gene transcription [4]. Infections by biofilm formation, following hip joint replacement, account for 7 % of all revision surgeries [5]. Such infections are difficult to detect, are tolerant to host defense mechanisms and antibiotics, and can lead to endocarditis [6]. A strategy to prevent or inhibit biomaterial-associated infection is to use materials which are resistant to bacterial infection [7]. There is evidence to suggest that a surface engineering strategy based on a coating comprised of zinc (Zn^{2+}), where ions elute in a controlled manner to the surface could reduce infection. Many pathogenic microorganisms mediate their resistance to inhibitory substances via biofilm formation [8]. Due to both the development of resistant

phenotypes [9], and the retarded penetration of antimicrobials into biofilms [10], approximately 10^4 higher doses of antimicrobials are needed to kill biofilms than for planktonic organisms. For biofilm formation to be inhibited in vivo, a biocide must be applied to the device prior to insertion [11]. Coatings have been produced based on chlorhexidine and silicone with ammonia couplings, but these have offered little clinical applicability due to erosion of the compounds in vivo [12, 13]. Although antibiotic treatment retards biofilm progression by eliminating planktonic cells, there is growing concern with cross-resistance exhibited by antibiotic-resistant strains to other antimicrobial agents such as disinfectants [14, 15]. A suitable agent should be effective against a broad range of Gram-positive and Gram-negative bacteria.

Bioglass was invented in the late 1960s and is now used clinically due to its ability to promote tissue regeneration [16]. Bioactive glasses can be formulated to contain and subsequently release clinically beneficial ions such as silver (Ag^+), zinc (Zn^{2+}), copper (Cu^{2+}) and gallium (Ga^{3+}) [17]. These ions can be released when the glass is in contact with aqueous medium, resulting in glass surface degradation. The release of such ions can prevent bacterial adhesion and inhibit biofilm formation [18]. It has also been suggested that bacterial depletion occurs due to an increasing pH and the subsequent osmotic effect, which results from ion release from glasses [19]. Recently, bioactive glasses containing Ga have attracted a great deal of attention related to the bactericidal and chemotherapeutic properties of the Ga^{3+} ion [20].

Elastomers have been widely used for composite fabrication due to their high capacity for filler loading. Poly(octanediol citrate) (POC) is a thermoset polyester elastomer which is made from non-toxic and inexpensive precursors by a simple polycondensation method [21]. The properties of POCs can be tailored by modifying both the initial monomer molar ratio and subsequent curing conditions [22]. The performance of POC can be improved by combining the polymer with a bioceramic phase such as hydroxyapatite or a bioactive glass [23, 24]. Bioactive glasses suffer from low fracture toughness and poor flexibility whereas polymers suffer from insufficient strength. Combining such materials can result in a composite with the synergistic advantages of both the polymeric phase and the bioactive glass.

The authors have previously reported on the fabrication and characterization of composite scaffolds formed from POC and a Ga/Zn ion-releasing glass for the purposes of hard tissue replacement and regeneration [23]. The physical and biological properties of these materials can be tailored by altering the amount of bioactive glass inclusion. It was found that Young's modulus of composites enhanced with increasing bioactive glass content within the matrix while in vitro degradation declined. There was found to be a threshold at which composites promoted osteoblast-like hFOB responses better than pure POC. Here we assess the release of Ga^{3+} and Zn^{2+} from these composite scaffolds and how this ion release influences bioactivity and antibacterial activity. To have a better understanding of ions release and migration to its surrounding, scaffold implanted bovine bone models were used.

2 Experimental sections

2.1 Composite scaffold fabrication

Composite scaffolds with various concentrations of melt-derived bioactive glass ($0.48SiO_2$–$0.12CaO$–$0.32ZnO$–$0.08Ga_2O_3$ molar fraction) were prepared by a porogen-leaching technique as previously described [23]. Briefly, POC pre-polymer was synthesized by addition of equimolar quantities of citric acid and 1,8-octanediol in a three-neck round bottom glass flask heated to 165 °C. After the mixture melted, the temperature was decreased to 140 °C and held for 1 h. The pre-polymer was dissolved in 1,4-dioxane to obtain a 20 % solution and then a defined amount of bioactive glass (10, 20 or 30 wt%) was added to the solution and sonicated for 30 min. The composite scaffolds thus obtained were named POC–BG-10 %, POC–BG-20 % and POC–BG-30 %. Subsequently, 90 wt% of salt porogen (NaCl) was added to the mixture and the resultant material was stored in an oven (80 °C, 7 days). When curing was complete, the blocks of POC–BG–NaCl were washed in distilled water for 4 days to remove the salts. Finally, the scaffolds were frozen (−80 °C) and cut to the required shape. The scaffolds were freeze-dried overnight before use.

2.2 Ion release study

The analysis of ion release was carried out by soaking 11–14 mg cylindrical composite scaffolds in 10 ml phosphate buffer saline (PBS, pH 7.4) in a conical flask. Samples were placed in an orbital shaker incubator for periods of 1, 7, 14, and 28 days. The scaffolds were taken out from PBS at timed intervals and the extracts were refrigerated (5 °C) prior to being analyzed by a plasma–atomic emission spectrometer (MP–AES) Agilent 4100 (Agilent Technologies, Inc., Santa Clara, CA, USA) for Si, Ca, Zn and Ga concentration measurement in the solutions.

2.3 Acellular in vitro tests in SBF

In vitro bioactivity was evaluated in an acellular simulated body fluid (SBF) prepared according to the method reported by Kokubo and Takadama [25]. Three replicates

for each sample of the cylindrical scaffolds (11–14 mg) were immersed separately in 20 ml SBF and incubated at 37 °C. At pre-determined time intervals (1, 7, 14 and 28 days) the samples were removed from the solutions and gently washed with distilled water and dried at 37 °C. Further, all the samples were analyzed by SEM–EDS for elemental composition and morphology. The ionic concentrations of extract solutions from the scaffolds were analyzed by inductively coupled plasma mass spectrometry (ICP-MS, Agilent 7500, USA).

2.4 In vitro bone tests for ion penetration into bone tissue matrix

Bovine bone specimens (2 cm × 2 cm × 1 cm) were sourced from a local butcher shop, cleaned by detaching any soft tissues using a cutter and a 5 mm hole was drilled through the center. The specimens were washed thoroughly with ultrapure water and then soaked in NaCl solution for 1 day. The as-prepared sterilized scaffolds (6 mm diameter × 6 mm height) were used to fill the voids of the bones. The specimens were immersed into PBS and incubated for 7 days at 37 °C. At day 7, specimens were removed from PBS and dried in a vacuum oven at 37 °C. A piece of bone was used for each scaffold, an unfilled sample of bone (without scaffold implantation) was used as a positive control and a sample of bone without incubation in PBS was used as a negative control. Further, X-ray microanalysis of the bone surface was performed to quantitatively characterize the concentration of ions taken up by the bone.

2.5 Scanning electron microscopy and energy disperse spectrometric analysis

Microanalysis was obtained using an energy dispersive spectrometer (EDS: 20 mm X-Max, Oxford Instruments, Oxford, UK) and the INCA software connected to a scanning electron microscope (SEM: Quanta™ 250 FEG—FEI, USA) at 20 kV. All scaffolds were gold-coated using a 150 rotary-pumped sputter coater (Quorum Technologies). All samples were analyzed in triplicate under the same microscopy conditions. Analysis was performed from the scaffold-bone interface onto the edge of bone specimen.

2.6 Antibacterial tests

Antibacterial tests were performed using a liquid culture method as a qualitative measure of cell growth. The growth of a gram negative (*Escherichia coli*, ATCC 15597) and a gram positive bacteria (*Staphylococcus aureus,* NCTC 6571) in LB broth in the presence of rectangular composite scaffolds (1 cm wide × 3 cm length) was investigated following 10 h incubation and the results compared with a pure LB broth culture as control. Before performing the test, the scaffolds were autoclaved at 126 °C and the monomer residues in scaffolds were washed in PBS followed by rinsing with distilled water in order to adjust the pH to physiological level. 50 µl of bacteria culture with the final cell density of approximately 10^5–10^6 colony forming unit per millimeter (CFU/ml) were inoculated in a 10 ml solution of autoclaved LB broth and constructs in a 15 ml conical tube. The tubes were incubated at 37 °C and shaken at 100 rpm using an orbital shaker incubator (Benchtop, Ind. & Vac. Instrument). The optical densities of the cultures were serially monitored every 2 h up to 10 h at 595 nm (OD 595) using a microplate reader (BMG LABTECH, Offenburg, Germany). In order to determine the viable bacteria, cultures (after 10 h) were diluted to 10^{-6} and placed on LB agar plates and incubated at 37 °C overnight. After incubation, the colonies were quantified and digital images of the plates were captured.

3 Results and discussion

3.1 Ion release study

The SiO_3^{2-}, Ca^{2+}, Zn^{2+} and Ga^{3+} ions release profiles of POC–BG composite scaffolds in PBS are presented in Fig. 1. Elemental concentration of all the components increased with time. As expected, all the composites showed a similar release trend with a statistically higher release of SiO_3^{2-} at every time point. The Ga^{3+} and Ca^{2+} ion release ratios were also found to increase over incubation time, with a maximum of 1.5 and 1.4 ppm, respectively. The increase in ionic concentration of SiO_3^{2-}, Ca^{2+} and Ga^{3+} with incubation time revealed that POC is degrading alongside the glass phase, in consistence with our previous study [23]. As composite scaffolds degraded over time, the medium was able to diffuse through the matrix thus causing more glass material to be released. Although a high Zn concentration is present in the glass series, very low concentrations of Zn^{2+} ions were recorded in the PBS solution over 1–28 days. The measured amounts (~0.03 ppm) were significantly lower than the reported average Zn^{2+} ion concentration of human plasma (0.95–1.30 ppm) and in vitro toxic levels (5.9 and 6.1 ppm) for murine osteoblasts and L929 fibroblast respectively till 28 days of immersion in PBS [26, 27]. It may reduce one of the concerns about the release of high level of Zn^{2+} which may cause cytotoxicity to cells.

3.2 Acellular in vitro test in SBF

Figure 2 shows the release of Ca^{2+}, PO_4^{3-}, SiO_3^{2-}, Zn^{2+} and Ga^{3+} ions in SBF on day 1, 7, 14 and 28 days. The

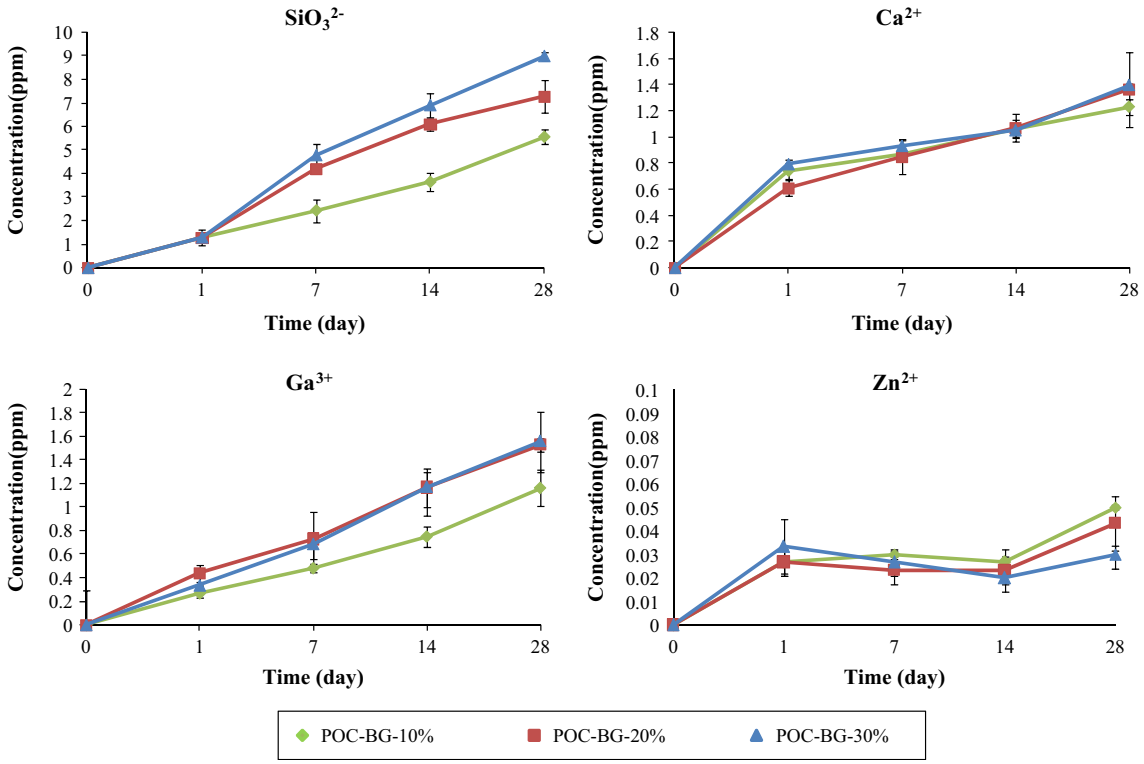

Fig. 1 Ion release kinetics from composite scaffolds in PBS: AES plots of elemental concentrations of SiO_3^{2-}, Ca^{2+}, Ga^{3+} and Zn^{2+} after 28 days of scaffolds immersion

experiment was performed to assess in vitro behavior of POC–BG-10 %, POC–BG-20 % and POC–BG-30 % in terms of chemical composition changes in the simulated body environment. The concentration of Ga^{3+} follows a steadily rising trend and POC–BG-30 % showed the highest Ga^{3+} release at pre-determined time points. At the end of the experiment, Ga^{3+} concentration from POC–BG-30 % extracts showed similar result observed for the ion release profile in PBS but not for POC–BG-10 % and POC–BG-20 %. However, the assessment of Zn^{2+} ion release revealed a higher concentration when compared to the study in PBS (Fig. 1), although the Zn^{2+} was still relatively low for the duration of the experiment, reaching a maximum of 0.24 ppm at day 28. There were no significant differences for SiO_3^{2-} concentration measured in PBS and SBF at any time-points. The Ca^{2+} concentration in SBF across all groups increased at day 1 and it could be concluded that an increase in Ca^{2+} concentration is induced by the release of Ca^{2+} ions from composites. At day 7, Ca^{2+} concentrations reached the lowest level and then gradually increased until the end of the experiment (day 28). A low decrease in Ca^{2+} concentration in the later stages are most likely a consequence of the consumption of Ca^{2+} through the formation of calcium phosphate (CaP) on scaffold surfaces. The concentration of PO_4^{3-} decreased when composite scaffolds were soaked and was less than original SBF phosphate concentration during the entire period of the experiment. The depletion of PO_4^{3-} from SBF confirms the formation of CaP layer on the scaffolds surfaces during incubation as presented in Fig. 3. The formation of a CaP surface layer is considered essential for the biological success of the material as it may determine the suitability of material as a bone substitute by the ability to chemically bond to the adjacent living bone [25]. Thus, from the results, an interaction between the SBF and the composites has occurred. SEM–EDS analysis confirmed the presence of CaP layers on the surfaces of the composite specimens. However, the CaP formation ability was poor. The very low CaP-forming ability can be attributed to release of both Zn^{2+} and Ga^{3+} from the composite scaffolds.

Although Zn is known to be a potent inhibitor of apatite crystal growth, it was found that Zn^{2+} release, at nontoxic levels, does not completely inhibit initial apatite deposition [28]. For example, Fuierer et al. reported that a low concentration of Zn^{2+} ions (0.25 ppm) was able to slow, but not stop, the rate of HA formation from supersaturated solutions by 78 % [29]. They found that pre-adsorbed Zn on the seed crystals was effective in retarding crystal growth as a result of formation of $Zn_2(PO_4)_3$ complexes. Zn initially retards HA nucleation and the number of nuclei decreases with the amount of Zn addition [30]. This

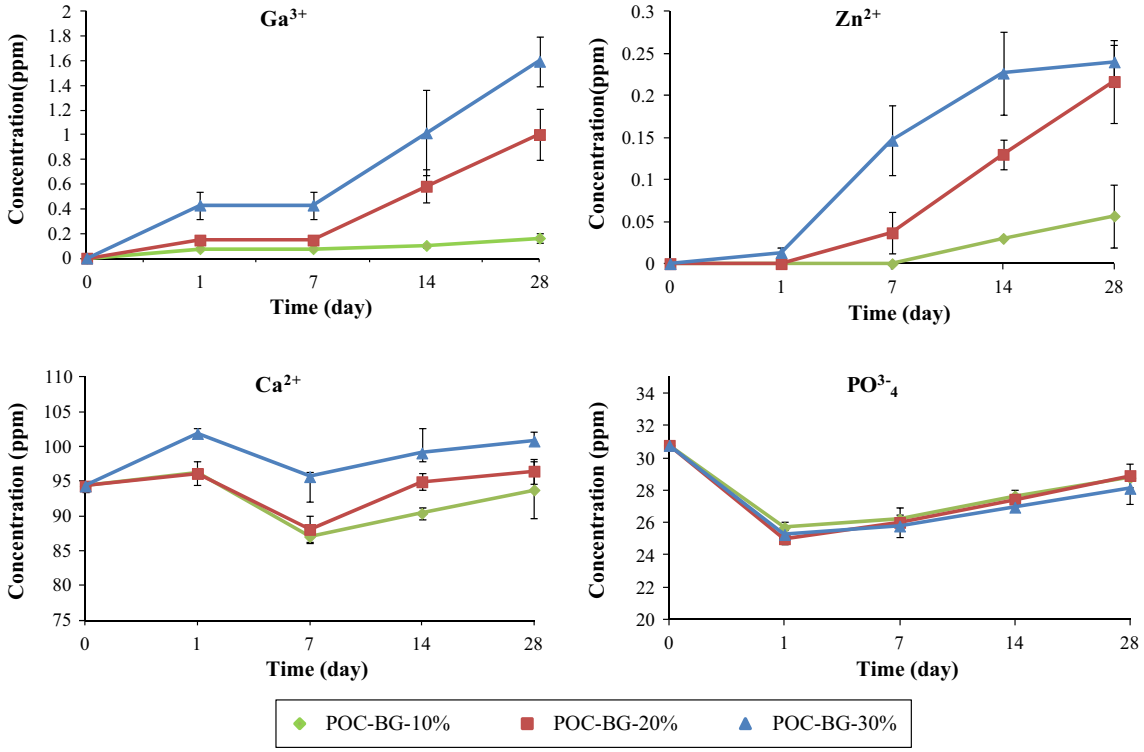

Fig. 2 In vitro ion release kinetics for composite scaffolds in SBF: ICP plots of elemental concentration of Ca^{2+}, PO_4^{3-}, Ga^{3+} and Zn^{2+} versus immersion time for the investigated composites

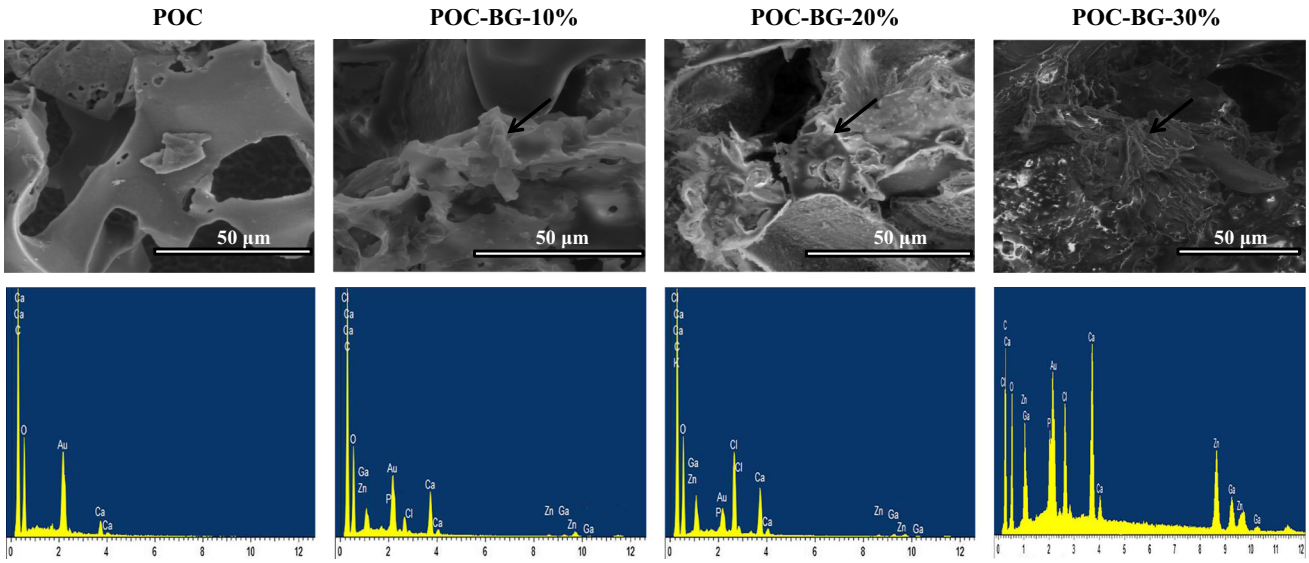

Fig. 3 *Top* SEM images confirm CaP layer deposition (*arrows*) on the composite scaffolds during immersion in SBF and (*bottom*) EDS profiles of the composite scaffolds after being soaked in SBF for 28 days

phenomenon was explained by the ability of Zn to deactivate the HA nuclei. When nucleation sites are reduced, the chance for each HA nucleus to receive Ca^{2+} and PO_4^{3-} in SBF will increase. As a result, larger HA crystals could be produced. At longer soaking times, the available Zn on the surface is covered by the HA layer and, due to the higher bond energy of Zn–O (rather than Ca–O), the diffusion of Zn from the network into the solution is retarded and its influence on HA formation reduces [30]. Moreover, it is understood that retarded HA formation of Zn-doped

bioactive glasses can further facilitate slower HA crystallization and thus provide a better bone bonding interface in vivo [31]. Indeed, the presence of Zn in the bioactive glass phase explains the lack of crystallinity associated with the formation of the apatite layers observed on composite scaffolds after immersion in SBF. Thus, the release of Zn^{2+} and its subsequent inclusion in the apatite layer favors the formation of amorphous apatite.

It has been also reported that Ga has an inhibitory effect on HA deposition and growth [32]. Ga-doped Brushite showed a reduced rate of HA formation in a solution containing Ca. This phenomenon is a result of Ga adsorption on the apatite surface which further prevents the growth of HA [33]. In addition, to observing the impact of Ga on bioactivity, Franchini et al. [34] examined a series of glasses based on 45S5 that contained increasing amounts of Ga up to 3.4 mol%. The bioactivity test in SBF revealed that there is a competition between Ca^{2+} and Ga^{3+} for binding with phosphate ions. As a result after long period of soaking the phosphate ions are not sufficient to precipitate with the continuously released Ca^{2+} from the glass to precipitate HA. Consequently the Ca/P ratio of SBF and glass exceed the topical Ca/P ratio of HA (1.67) and carbonate ions from SBF begin to form calcite. It is hypothesized that this replacement can inhibit crystallite growth [34]. Overall, the co-precipitation of Ga–phosphate might be partially responsible for delayed CaP precipitation [35]. Ga may also act as a network former in the glass and consequently can reduce the solubility of the glass which will retard bioactivity [35]. In addition, the increased acidity caused by Ga-containing bioactive glasses may be another reason for delayed apatite formation [35]. The enhanced surface acidity of Ga-containing glass is expected to preliminary inhibit the deposition of CaP, the essential prerequisite for HA crystallization. In the present study, the release of both Zn and Ga can extremely inhibit apatite formation and crystallization such that after 28 days of incubation in SBF it was still only partially covered by a CaP layer.

3.3 In vitro bone tests for ion penetration into bone tissue matrix

The digital image of a selected bovine bone implanted scaffold and the corresponding SEM image are shown in Fig. 4. The specimens were examined by EDS at the predetermined distances after 7 days soaking in PBS (Fig. 4) and the results are presented in Fig. 5. Four points at various distances from the scaffold-bone interface (i.e. 0, 200, 1500 and 4500 μm) were investigated by EDS for the presence of all ionic species from the bioactive glass phase in the composite. Very low concentrations of Ga^{3+} (approximately 0.06 %) were absorbed into the bone from the specimens containing POC–BG-20 % and POC–BG-30 % scaffolds by up to 1500 μm from the implanted scaffolds. The highest Zn^{2+} concentration was detected at point 0 and it decreased with distance from the scaffold. The results demonstrate that Zn^{2+} ions were released from the scaffolds and taken up into the bone as far as 4.5 mm away from the implant. As expected, Zn^{2+} was not detected for the unfilled POC and control specimens.

The amounts of Ca^{2+} and PO_4^{3-}, alongside the Ca/P ratio, were determined at all points (Fig. 5). Significantly higher Ca^{2+} and PO_4^{3-} ionic concentrations to Zn^{2+} were detected at all points in the bone specimens and were attributed predominantly to the bone itself. PO_4^{3-} ionic concentration remained relatively constant in the observed area. The concentration of Ca^{2+} slightly decreased in the vicinity of the bone-scaffold interface as Zn^{2+} is incorporated into the bone. The observed patterns of Zn^{2+} and Ca^{2+} migration into bone specimens are consistent with a study by Wren et al. [36]. However it is unclear whether the reduction in Ca^{2+} concentration was significant, since EDS is predominantly a qualitative tool and it cannot distinguish between low counts [36]. Furthermore, higher Ca^{2+} was detected at the bone-scaffold interface for POC–BG-10 % compared to POC–BG-20 % and POC–BG-30 % which can be attributed to the lower Zn^{2+} concentration recorded for the POC–BG-10 % composite. As can be seen in Fig. 4, no significant difference in Ca/P ratio was observed between any of the samples (calculated at approximately 1.3—1.5). This shows that incorporation of Zn^{2+} in bone does not influence the original Ca/P ratio of the mineral phase of bone. Although the theoretical fraction of Ca and P of bone should be 40.3 and 18.4 % respectively, it can vary and is influenced by factors such as bone source, location and age as well as the presence of metabolic bone disease [37, 38].

Comparison of results from the ion release study in PBS and scaffold implanted bones reveals that Zn^{2+} is released from composite scaffolds and quickly re-precipitated in bones while Ga^{3+} can be recorded in acceptable concentrations in buffer solutions. A possible mechanism for this is the dissolution of Zn^{2+} and $ZnOH^{+}$ ions from the glass particles and precipitation of the hydroxide, $Zn(OH)_2$, onto the bone surface [39]. It may also be the reason for the low levels of Zn^{2+} observed in the extracts from the ion release experiments. Foley and Blackwell also observed that the highest rate of Zn^{2+} release from zinc phosphate cements occurred after 2 days, and reached almost zero after 28 days of incubation [40]. Similarly, the highest rate of Zn^{2+} release detected by Osinaga et al. was within 24 h [41].

The Zn^{2+} ion is known to have a stimulatory influence on bone formation and mineralization and an inhibitory influence on bone resorption [42]. Zn deficiency is a common reason for bone growth retardation due to

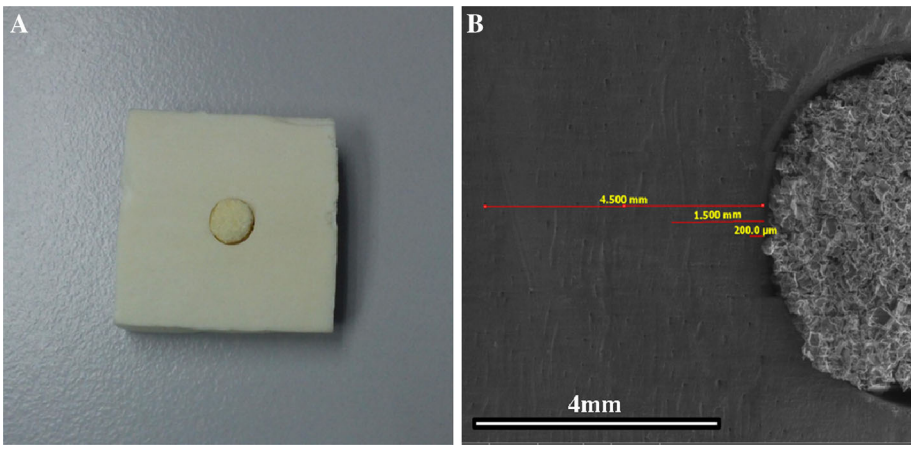

Fig. 4 **a** Digital image and **b** SEM image of POC scaffold implanted into bone specimen

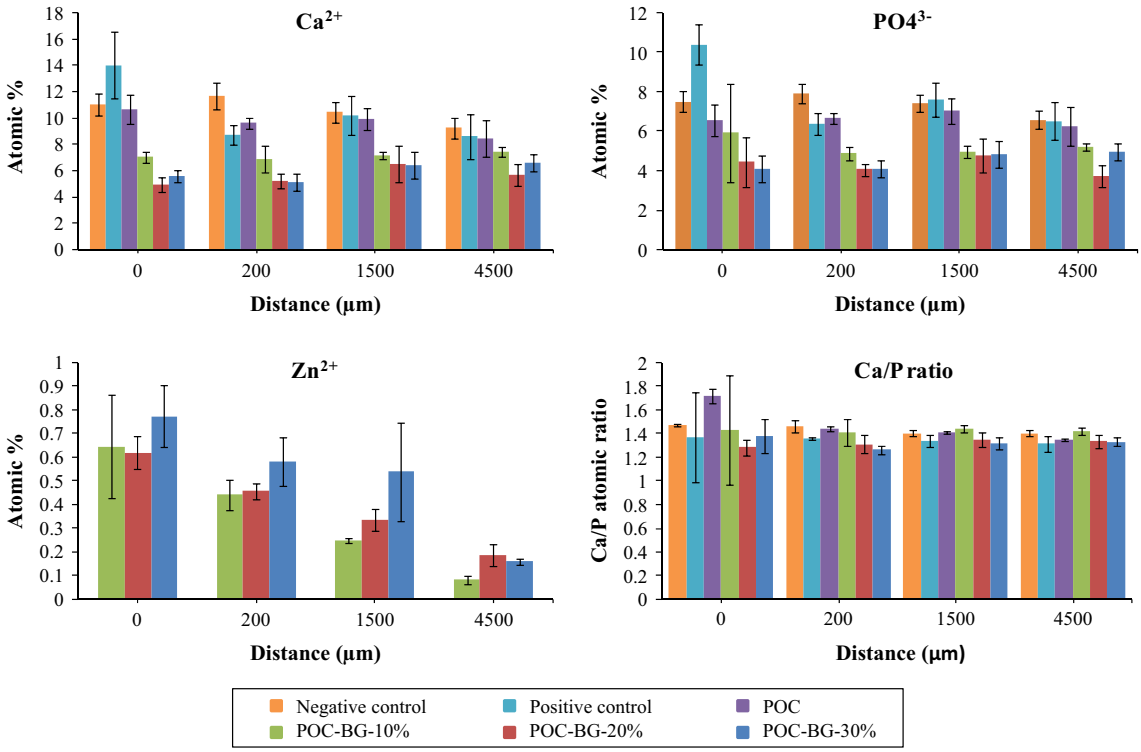

Fig. 5 Normal atomic % EDS data for Ca, P and Zn content as well as Ca/P ratio at scaffold-bone interface at various distances 0, 200, 1500 and 4500 µm (Color figure online)

reduction in osteoblastic activity, in collagen content, in proteoglycan synthesis, and in alkaline phosphatase (ALP) activity [43]. Low Zn bioavailability can also lead to inadequate immunoresistance to infections in the elderly [44]. It has been found that osteoporotic patients have a lower skeletal Zn content than normal [45]. Excessive Zn content can also result in disorders such as growth retardation, anaemia and immunosuppression [44]. Thus, the beneficial effect of Zn is greatly dependent upon its dose and duration. It is also expected that the local delivery of Zn would have a significant impact on bone regeneration. The levels of synergistic ion release from our materials correlates well with the levels of Ga^{3+} and Zn^{2+} ions typically associated with clinical benefits (cell responses). The release of both ions at nontoxic level from our materials could be the main reason for improving the cell proliferation and increasing collagen synthesis which are reported in our previous study [23].

3.4 Antibacterial tests

The effect of bioactive glass addition on the growth of both *E. coli* and *S. aureus* was investigated by monitoring culture turbidity for 10 h. The results are shown in Figs. 6 and

7. It can be seen that the culture containing POC is slightly different from that of the negative control (LB broth) after 10 h. The low antibacterial activity of POC may be attributed to the presence of a large number of acid groups. As shown in Fig. 6, the results indicate that both *E. coli* and *S. aureus* growth were significantly inhibited by the addition of bioactive glass. As the value of the optical density (OD) at 595 nm represents the absorbance of the bacteria, a decrease in OD implies bacterial depletion [46]. Consequently, the antibacterial efficacy of the materials was enhanced in proportion to the bioactive glass concentration. In particular, the culture including composite with 30 wt% bioactive glass inclusion had significantly less bacteria than the control during incubation at 37 °C. These data suggest that the antibacterial activity of composite scaffolds is dependent on glass content.

Growing cultures after 10 h of growth were also plated to count viable cells, and the viable cell numbers are consistent with the OD of the growing cultures (Fig. 7). Notably, at that time point, "viable cells recovered" decreased significantly with increasing glass content. As shown in Fig. 8, POC–BG-30 % scaffolds effectively limited the growth of both *E. coli* and *S. aureus*. Antibacterial testing against *E. coli* and *S. aureus* revealed bacteriostatic effects. However, the antibacterial activity of the composite scaffolds against *E. coli* was not as effective as that on *S. aureus*. This result might be attributed to the differences on membrane structure and composition of the examined bacteria; *S. aureus*, a typical Gram-positive bacterium, is composed of a peptidoglycan layer which is a loosely-packed network structure with plenty of pores. Through these pores, foreign molecules can be transported across the cell into the interior with little obstruction. In contrast, *E. coli* is a typical Gram-negative bacterium which due to the presence of lipopolysaccharide molecule contains an outer membrane outside the porous peptidoglycan layer acting as drug barrier. The barrier can resist the permeation of large foreign molecules [47]. Thus, our composite scaffolds would be expected to have different

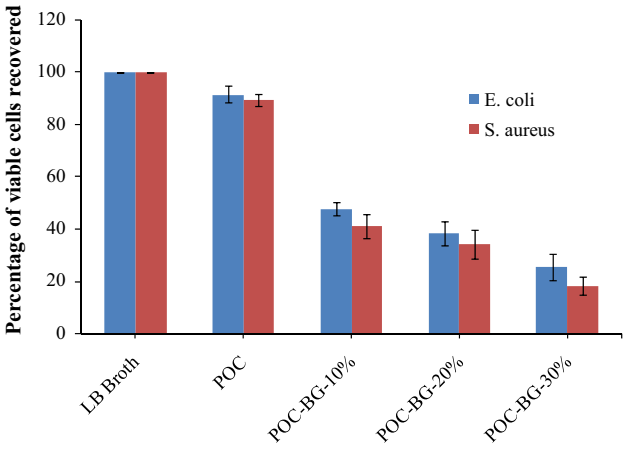

Fig. 7 The viable *E. coli* and *S. aureus* recovered from agar plates after 10 h of incubation at 37 °C (Color figure online)

antibacterial activity against these two bacteria due to the ions release.

The antimicrobial effect of bioactive glasses is most likely a consequence of an ion release effect, in addition to pH changes that they induce [48]. It is postulated that the antimicrobial effect of the composite scaffolds is based on the release of metal ions (Ga^{3+} and Zn^{2+}) to the cultures. Bioactive glasses doped with Ga^{3+} have antibacterial activity against both Gram-positive (*Staphylococcus aureus, methicillin-resistant Staphylococcus aureus*, and *Clostridium difficile*) and Gram-negative (*Escherichia coli* and *Pseudomonas aeruginosa*) bacteria [20]. Due to the similarity of Ga^{3+} and Fe^{3+} in terms of ionic radius, coordination number and electronegativity, Ga^{3+} (redox inactive) can efficiently compete with Fe^{3+} (redox active) for binding to iron-containing enzymes, as well as to transferrin, lactoferrin, and microbial iron chelators [34, 49]. However, under the same conditions, unlike Fe^{3+}, Ga^{3+} cannot be reduced leading to inhibition of a number of essential biological reactions including those responsible for DNA and protein synthesis as well as energy production [50, 51]. Since only one-third of circulating transferrin is

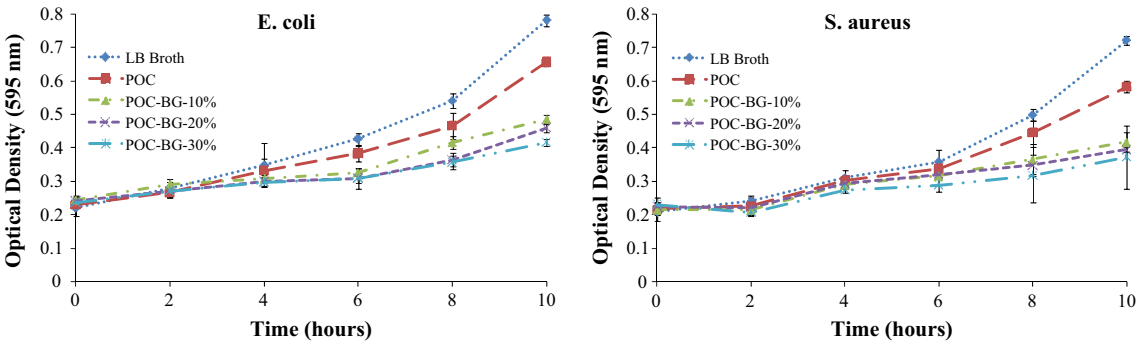

Fig. 6 Effect of the composite scaffolds on the growth of *E. coli* and *S. aureus*; measured by monitoring the optical density at 595 nm

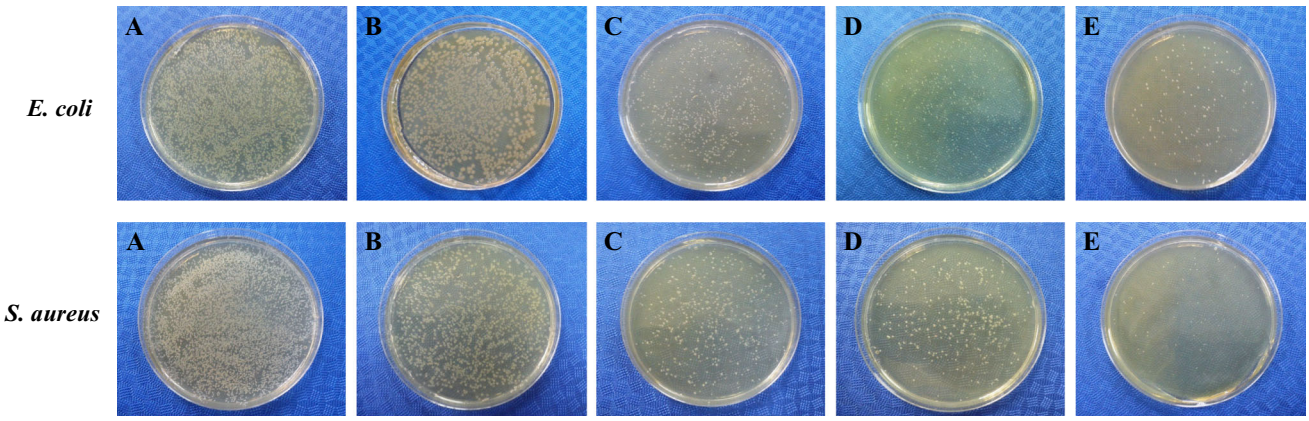

Fig. 8 Plate assay of *E. coli* and *S. aureus* using **a** LB broth; **b** POC; **c** POC–BG-10 %; **d** POC–BG-20 %; **e** POC–BG-30 % at 10 h

occupied by iron, Ga^{3+} can react with the remaining sites and form transferring-Ga complexes and diminish the bacterial uptake of Fe^{3+} as well as the enhancement of a microorganism's vulnerability [51]. Recently, it has been reported that low concentrations of Ga^{3+} inhibit biofilm formation from *E. coli* and *S. aureus* even when a high percentage of bacteria have survived the Ga_2O_3 treatment [52]. An explanation for this behavior is that Ga^{3+} decreased bacterial Fe^{3+} uptake in a concentration-dependent manner.

Recent reports have shown that Zn in micromolar concentrations can inhibit biofilm formation from several Gram-positive and negative bacteria [53]. The antibacterial activity of Zn^{2+} against *Streptococcus mutans* and *Actinomycesviscosus* was found to be a result of Zn^{2+} migration [54]. The antibacterial activity of Zn^{2+} depends on its concentration and contact duration. Two distinct mechanisms of actions have been proposed to explain the antimicrobial activities of Zn^{2+} leading to cell death:

(1) a direct interaction with microorganism membrane proteins leading to membrane destabilization and enhanced permeability and finally destruction of their capability to transport through the plasma membrane;
(2) an interaction with nucleic acids and deactivation of enzymes of the respiratory system and electron transport system [55, 56].

It is reported that Gram-positive bacteria were the most susceptible bacterial group to Zn^{2+} but Gram-negative aerobic bacteria were usually not inhibited even at high concentrations (1024 µl/ml) [57]. However, Alhalawani et al. found that, in a glass series containing both Ga and Zn, the antibacterial activity was improved by the release of Zn^{2+} ions and not by Ga^{3+} ions [58]. It was found that the glass with lower Ga^{3+} content showed enhanced antibacterial properties against *E. coli*. Thus, in the work reported here, release of Zn^{2+} ions may be the reason for significant antibacterial activity of the composites against both Gram-positive and Gram-negative bacteria.

The release of both Ga^{3+} and Zn^{2+} ions at a controlled rate, could offer significantly enhanced biological performance of materials for bone tissue regeneration. It has been reported that Ga^{3+} and Zn^{2+} in specific concentrations show therapeutic effects on the growth and proliferation of osteoblastic cells [59, 60]. Therefore, these ions doped to bioactive glasses with the aim of promoting bone forming ability as well as achieving anti-bacterial and anti-inflammatory properties. Our previous study revealed that the composite scaffold containing 10 % bioactive glass showed higher cell attachment and type-I and type-III collagen synthesis compared to composites with 20 and 30 % bioactive glass. The findings in the present study indicate that adding the bioactive glass into the matrix improved the bacteriostatic properties of composites and the intensity of those effects corresponds with glass content in the composite. Thus, composites with bioactive glass containing therapeutic ions could not only improve antibacterial properties but also are expected to improve cell adhesion and proliferation. However, there is theoretically a threshold of glass content at which most of the desirable properties can be satisfactorily achieved. Our findings present a new approach in the production of tissue engineering scaffolds which would eventually enable a minimal risk of infection and reduce the need for revision surgery.

4 Conclusion

In this study, composite scaffolds of POC and bioactive glass containing Ga and Zn were fabricated and evaluated for solubility, bioactivity and antibacterial activity. Ion release into both PBS and SBF revealed that Ga^{3+} release was similar in both solutions while Zn^{2+} release was slightly higher in SBF after 28 days of incubation. It was

found that apatite formation was significantly inhibited due to the release of these ions from composite scaffolds. In a bovine bone model, it was found that Zn^{2+} was released and penetrated into the bones by as far as 4500 μm from the scaffold-bone interface. However, the presence of Zn^{2+} on the bone surface did not affect Ca/P ratio at the measured points. The resulting composite scaffolds were found to be highly reactive against both Gram-positive *S. aureus* and Gram-negative *E. coli* bacteria. The antibacterial activity of composites increased with glass concentration. It was found that the bacteria were significantly inhibited by the release of Zn^{2+} and Ga^{3+} ions. If these results can be confirmed in vivo, then composite scaffolds of elastomers and bioactive glasses containing clinically beneficial ions such as Zn^{2+} and Ga^{3+} may have applicability in bone grafting due to their antibacterial activity and simultaneous bone tissue formation. Further research is needed to evaluate possible synergistic effects of released metal ions, especially Ga^{3+} and Zn^{2+}, on biological response.

Acknowledgments This research is supported by a High Impact Research Grant (UM.C/625/1/HIR/MOHE/ENG/58) from the Ministry of Higher Education Malaysia and University of Malaya Research Grant (UMRG, RG156-12AET).

References

1. Alvarez K, Nakajima H. Metallic scaffolds for bone regeneration. Materials. 2009;2(3):790–832. doi:10.3390/ma2030790.
2. Puppi D, Chiellini F, Piras AM, Chiellini E. Polymeric materials for bone and cartilage repair. Prog Polym Sci. 2010;35(4):403–40. doi:10.1016/j.progpolymsci.2010.01.006.
3. Belt HVd, Neut D, Schenk W, Horn JRV, Mei HCVD, Busscher HJ. Infection of orthopedic implants and the use of antibiotic-loaded bone cements: a review. Acta Orthop. 2001;72(6):557–71. doi:10.1080/000164701317268978.
4. Donlan RM, Costerton JW. Biofilms: survival mechanisms of clinically relevant microorganisms. Clin Microbiol Rev. 2002;15(2):167–93. doi:10.1128/CMR.15.2.167-193.2002.
5. Malchau H, Meeting AAOOS. Prognosis of total hip replacement: update of results and risk-ratio. Analysis for Revision and Re-revision from the Swedish National Hip Arthroplasty Register 1979–2000. 2002.
6. Stewart PS, Costerton JW. Antibiotic resistance of bacteria in biofilms. Lancet. 2001;358(9276):135–8. doi:10.1016/S0140-6736(01)05321-1.
7. Campoccia D, Montanaro L, Arciola CR. A review of the clinical implications of anti-infective biomaterials and infection-resistant surfaces. Biomaterials. 2013;34(33):8018–29. doi:10.1016/j.biomaterials.2013.07.048.
8. Chaieb K, Mahdouani K, Bakhrouf A. Detection of icaA and icaD loci by polymerase chain reaction and biofilm formation by Staphylococcus epidermidis isolated from dialysate and needles in a dialysis unit. J Hosp Infect. 2005;61(3):225–30. doi:10.1016/j.jhin.2005.05.014.
9. Brown M, Gilbert P. Sensitivity of biofilms to antimicrobial agents. J Appl Bacteriol. 1993;74(S22):87S–97S. doi:10.1111/j.1365-2672.1993.tb04345.x.
10. Stewart PS. Mechanisms of antibiotic resistance in bacterial biofilms. Int J Med Microbiol. 2002;292(2):107–13. doi:10.1078/1438-4221-00196.
11. Meyer B. Approaches to prevention, removal and killing of biofilms. Int Biodeter Biodegr. 2003;51(4):249–53. doi:10.1016/S0964-8305(03)00047-7.
12. Logghe C, Van Ossel C, D'Hoore W, Ezzedine H, Wauters G, Haxhe J-J. Evaluation of chlorhexidine and silver-sulfadiazine impregnated central venous catheters for the prevention of bloodstream infection in leukaemic patients: a randomized controlled trial. J Hosp Infect. 1997;37(2):145–56. doi:10.1016/S0195-6701(97)90184-5.
13. Gottenbos B, van der Mei HC, Klatter F, Nieuwenhuis P, Busscher HJ. In vitro and in vivo antimicrobial activity of covalently coupled quaternary ammonium silane coatings on silicone rubber. Biomaterials. 2002;23(6):1417–23. doi:10.1016/S0142-9612(01)00263-0.
14. Cerca N, Martins S, Cerca F, Jefferson KK, Pier GB, Oliveira R, et al. Comparative assessment of antibiotic susceptibility of coagulase-negative staphylococci in biofilm versus planktonic culture as assessed by bacterial enumeration or rapid XTT colorimetry. J Antimicrob Chemother. 2005;56(2):331–6. doi:10.1093/jac/dki217.
15. Langsrud S, Sidhu MS, Heir E, Holck AL. Bacterial disinfectant resistance—a challenge for the food industry. Int Biodeter Biodegr. 2003;51(4):283–90. doi:10.1016/S0964-8305(03)00039-8.
16. Hench LL, Splinter RJ, Allen W, Greenlee T. Bonding mechanisms at the interface of ceramic prosthetic materials. J Biomed Mater Res. 1971;5(6):117–41. doi:10.1002/jbm.820050611.
17. Kaur G, Pandey OP, Singh K, Homa D, Scott B, Pickrell G. A review of bioactive glasses: their structure, properties, fabrication and apatite formation. J Biomed Mater Res A. 2014;102(1):254–74. doi:10.1002/jbm.a.34690.
18. Kaneko Y, Thoendel M, Olakanmi O, Britigan BE, Singh PK. The transition metal gallium disrupts *Pseudomonas aeruginosa* iron metabolism and has antimicrobial and antibiofilm activity. J Clin Invest. 2007;117(4):877. doi:10.1172/JCI30783.
19. Stoor P, Söderling E, Salonen JI. Antibacterial effects of a bioactive glass paste on oral microorganisms. Acta Odontol Scand. 1998;56(3):161–5. doi:10.1080/000163598422901.
20. Valappil SP, Ready D, Neel EAA, Pickup DM, Chrzanowski W, O'Dell LA, et al. Antimicrobial gallium-doped phosphate-based glasses. Adv Funct Mater. 2008;18(5):732–41. doi:10.1002/adfm.200700931.
21. Yang J, Webb AR, Ameer GA. Novel citric acid-based biodegradable elastomers for tissue engineering. Adv Mater. 2004;16(6):511–6. doi:10.1002/adma.200306264.
22. Yang J, Webb AR, Pickerill SJ, Hageman G, Ameer GA. Synthesis and evaluation of poly (diol citrate) biodegradable elastomers. Biomaterials. 2006;27(9):1889–98. doi:10.1016/j.biomaterials.2005.05.106.
23. Zeimaran E, Pourshahrestani S, Pingguan-Murphy B, Kadri NA, Rothan HA, Yusof R, et al. Fabrication and characterization of poly (octanediol citrate)/gallium-containing bioglass microcomposite scaffolds. J Mater Sci. 2015;50:1–13. doi:10.1007/s10853-014-8782-2.
24. Qiu H, Yang J, Kodali P, Koh J, Ameer GA. A citric acid-based hydroxyapatite composite for orthopedic implants. Biomaterials. 2006;27(34):5845–54. doi:10.1016/j.biomaterials.2006.07.042.
25. Kokubo T, Takadama H. How useful is SBF in predicting in vivo bone bioactivity? Biomaterials. 2006;27(15):2907–15. doi:10.1016/j.biomaterials.2006.01.017.
26. Lansdown A. Zinc in the healing wound. Lancet. 1996;347(9003):706–7. doi:10.1016/S0140-6736(96)90072-0.
27. Yamamoto A, Honma R, Sumita M. Cytotoxicity evaluation of 43 metal salts using murine fibroblasts and osteoblastic cells.

J Biomed Mater Res. 1998;39(2):331–40. doi:10.1002/(SICI)1097-4636(199802)39:2<331:AID-JBM22>3.0.CO;2-E.
28. Ito A, Kawamura H, Otsuka M, Ikeuchi M, Ohgushi H, Ishikawa K, et al. Zinc-releasing calcium phosphate for stimulating bone formation. Mater Sci Eng, C. 2002;22(1):21–5.
29. Fuierer TA, LoRe M, Puckett SA, Nancollas GH. A mineralization adsorption and mobility study of hydroxyapatite surfaces in the presence of zinc and magnesium ions. Langmuir. 1994;10(12):4721–5. doi:10.1021/la00024a054.
30. Du RL, Chang J, Ni SY, Zhai WY, Wang JY. Characterization and in vitro bioactivity of zinc-containing bioactive glass and glass-ceramics. J Biomater Appl. 2006;20(4):341–60. doi:10.1177/0885328206054535.
31. Boyd D, Towler M, Wren A, Clarkin O, Tanner D. TEM analysis of apatite surface layers observed on zinc based glass polyalkenoate cements. J Mater Sci. 2008;43(3):1170–3. doi:10.1007/s10853-007-2362-7.
32. Blumenthal NC, Cosma V, Levine S. Effect of gallium on thein vitro formation, growth, and solubility of hydroxyapatite. Calcif Tissue Int. 1989;45(2):81–7. doi:10.1007/BF02561406.
33. Korbas M, Rokita E, Meyer-Klaucke W, Ryczek J. Bone tissue incorporates in vitro gallium with a local structure similar to gallium-doped brushite. J Biol Inorg Chem. 2004;9(1):67–76. doi:10.1007/s00775-003-0497-9.
34. Franchini M, Lusvardi G, Malavasi G, Menabue L. Gallium-containing phospho-silicate glasses: synthesis and in vitro bioactivity. Mater Sci Eng, C. 2012;32(6):1401–6. doi:10.1016/j.msec.2012.04.016.
35. Aina V, Morterra C, Lusvardi G, Malavasi G, Menabue L, Shruti S, et al. Ga-modified (Si–Ca–P) sol-gel glasses: possible relationships between surface chemical properties and bioactivity. J Phys Chem C. 2011;115(45):22461–74. doi:10.1021/jp207217a.
36. Wren A, Boyd D, Thornton R, Cooney J, Towler M. Antibacterial properties of a tri-sodium citrate modified glass polyalkenoate cement. J Biomed Mater Res B. 2009;90(2):700–9. doi:10.1002/jbm.b.31337.
37. Kuhn LT, Grynpas MD, Rey CC, Wu Y, Ackerman JL, Glimcher MJ. A comparison of the physical and chemical differences between cancellous and cortical bovine bone mineral at two ages. Calcif Tissue Int. 2008;83(2):146–54. doi:10.1007/s00223-008-9164-z.
38. Grynpas M, Pritzker K, Hancock R. Neutron activation analysis of bulk and selected trace elements in bones using a low flux SLOWPOKE reactor. Biol Trace Elem Res. 1987;13(1):333–44. doi:10.1007/BF02796644.
39. Pasquet J, Chevalier Y, Pelletier J, Couval E, Bouvier D, Bolzinger M-A. The contribution of zinc ions to the antimicrobial activity of zinc oxide. Colloid Surface A. 2014;457:263–74. doi:10.1016/j.colsurfa.2014.05.057.
40. Foley J, Blackwell A. In vivo cariostatic effect of black copper cement on carious dentine. Caries Res. 2002;37(4):254–60. doi:10.1159/000070867.
41. Osinaga PW, Grande RHM, Ballester RY, Simionato MRL, Rodrigues CRMD, Muench A. Zinc sulfate addition to glass-ionomer-based cements: influence on physical and antibacterial properties, zinc and fluoride release. Dental Mater. 2003;19(3):212–7. doi:10.1016/S0109-5641(02)00032-5.
42. Yamaguchi M. Role of zinc in bone formation and bone resorption. J Trace Elem Exp Med. 1998;11(2–3):119–35. doi:10.1002/(SICI)1520-670X(1998)11:2/3<119:AID-JTRA5>3.0.CO;2-3.
43. Calhoun NR, Smith JC Jr, Becker KL. The role of zinc in bone metabolism. Clin Orthop Relat R. 1974;103:212–34. doi:10.1097/00003086-197409000-00084.
44. Ripa S, Ripa R. Zinc and immune function. Minerva Med. 1994;86(7–8):315–8.
45. Reginster J-Y, Strause L, Saltman P, Franchimont P. Trace elements and postmenopausal osteoporosis: a preliminary report of decreased serum manganese. Med Sci Res. 1988;16:337–338.
46. Zhang L, Jiang Y, Ding Y, Povey M, York D. Investigation into the antibacterial behaviour of suspensions of ZnO nanoparticles (ZnO nanofluids). J Nanopart Res. 2007;9(3):479–89. doi:10.1007/s11051-006-9150-1.
47. Don T-M, Chen C-C, Lee C-K, Cheng W-Y, Cheng L-P. Preparation and antibacterial test of chitosan/PAA/PEGDA bilayer composite membranes. J Biomat Sci-Polym E. 2005;16(12):1503–19. doi:10.1163/156856205774576718.
48. Gubler M, Brunner T, Zehnder M, Waltimo T, Sener B, Stark W. Do bioactive glasses convey a disinfecting mechanism beyond a mere increase in pH? Int Endod J. 2008;41(8):670–8. doi:10.1111/j.1365-2591.2008.01413.x.
49. Pickup D, Moss R, Qiu D, Newport R, Valappil S, Knowles J, et al. Structural characterization by x-ray methods of novel antimicrobial gallium-doped phosphate-based glasses. J Chem Phys. 2009;130:064708. doi:10.1063/1.3076057.
50. Bernstein LR. Mechanisms of therapeutic activity for gallium. Pharmacol Rev. 1998;50(4):665–82.
51. Chitambar CR. Medical applications and toxicities of gallium compounds. Int J Environ Res Public Health. 2010;7(5):2337–61. doi:10.3390/ijerph7052337.
52. Murthy PS, Venugopalan V, Sahoo P, Dhara S, Das A, Tyagi A, et al. editors. Gallium oxide nanoparticle induced inhibition of bacterial adhesion and biofilm formation. IEEE International Conference on Nanoscience, Engineering and Technology (ICONSET); 2011.
53. Wu C, Labrie J, Tremblay Y, Haine D, Mourez M, Jacques M. Zinc as an agent for the prevention of biofilm formation by pathogenic bacteria. J Appl Microbiol. 2013;115(1):30–40. doi:10.1111/jam.12197.
54. Boyd D, Li H, Tanner D, Towler M, Wall J. The antibacterial effects of zinc ion migration from zinc-based glass polyalkenoate cements. J Mater Sci-Mater M. 2006;17(6):489–94. doi:10.1007/s10856-006-8930-6.
55. Fang M, Chen J-H, Xu X-L, Yang P-H, Hildebrand HF. Antibacterial activities of inorganic agents on six bacteria associated with oral infections by two susceptibility tests. Int J Antimicrob Agent. 2006;27(6):513–7. doi:10.1016/j.ijantimicag.2006.01.008.
56. Stanić V, Dimitrijević S, Antić-Stanković J, Mitrić M, Jokić B, Plećaš IB, et al. Synthesis, characterization and antimicrobial activity of copper and zinc-doped hydroxyapatite nanopowders. Appl Surf Sci. 2010;256(20):6083–9. doi:10.1016/j.apsusc.2010.03.124.
57. Söderberg TA, Sunzel B, Holm S, Elmros T, Hallmans G, Sjöberg S. Antibacterial effect of zinc oxide in vitro. Scand J Plast Recons. 1990;24(3):193–7. doi:10.3109/02844319009041278.
58. Alhalawani AM, Placek L, Wren AW, Curran DJ, Boyd D, Towler MR. Influence of gallium on the surface properties of zinc based glass polyalkenoate cements. Mater Chem Phys. 2014;147(3):360–4. doi:10.1016/j.matchemphys.2014.06.020.
59. Verron E, Masson M, Khoshniat S, Duplomb L, Wittrant Y, Baud'huin M, et al. Gallium modulates osteoclastic bone resorption in vitro without affecting osteoblasts. Brit J Pharmacol. 2010;159(8):1681–92. doi:10.1111/j.1476-5381.2010.00665.x.
60. Balamurugan A, Balossier G, Kannan S, Michel J, Rebelo AH, Ferreira JM. Development and in vitro characterization of sol–gel derived CaO–P 2 O 5–SiO 2–ZnO bioglass. Acta Biomater. 2007;3(2):255–62. doi:10.1016/j.actbio.2006.09.005.